

Ordered Sequence Detection and Robust Pulse Interval Modulation for IM/DD Based Optical Wireless Communications

Shuaishuai Guo, *Member, IEEE*, Ki-Hong Park, *Member, IEEE*, and Mohamed-Slim Alouini, *Fellow, IEEE*

Abstract—Digital pulse interval modulation (DPIM) is an advanced energy-efficient modulation techniques for optical wireless communications (OWC) based on intensity modulation with direct detection (IM/DD). DPIM requires no accurate symbol-level synchronization. It is capable of leveraging less slots to carry the same information as pulse position modulation (PPM) and thus more efficient than PPM. However, error propagation hampers the application of DPIM. Motivated by controlling error propagation, this paper proposes an ordered sequence detection (OSD) for DPIM. To detect a packet consisting of L -chips, the computational complexity of OSD is low, of the order $\mathcal{O}(L^2)$. Moreover, this paper also proposes a robust pulse interval modulation (RPIM) scheme with OSD. In RPIM, the last of every K symbols is with more power to transmit information and simultaneously to provide a built-in synchronization signal. In this way, error propagation is bounded in a slot of K symbols. Together with interleaver and forward error correction (FEC) code, the bit error rate (BER) can be greatly reduced. We derive the approximate uncoded BER performance of conventional DPIM with OSD and the newly proposed RPIM with OSD based on order statistic theory. We calculate the optimal power allocation in every K symbol slots minimizing the uncoded BER by using a bisection search algorithm. Simulations are conducted to collaborate on theoretical analysis. Optimal parameter settings are also investigated in uncoded and coded systems by simulations. Simulation results show that RPIM with OSD considerably outperforms existing DPIM with optimal threshold detection in either uncoded or coded systems over various channels.

Index Terms—Optical wireless communication, intensity modulation with direct detection (IM/DD), digital pulse interval modulation, ordered sequence detection, robust pulse interval modulation, bit error rate (BER)

I. INTRODUCTION

Intensity modulation with direct detection (IM/DD) is the most widely applied transmission scheme for optical wireless communication (OWC) by virtue of its low-complexity low-cost implementation [1]–[3]. The simplest intensity modulation is on-off keying (OOK). OOK modulates the data by leveraging the presence and absence of light pulse in a symbol interval [4]. It has relatively poor spectral efficiency and energy efficiency. To improve its spectral efficiency, M -ary pulse amplitude modulation (M -PAM) is introduced to carry more information bits per channel use. Despite M -PAM can improve its spectrum efficiency by increasing M , its energy efficiency is still relatively low. In addition, both OOK and M -PAM have to tackle dynamic detection threshold problem, which necessarily requires the channel state information at the receiver (CSIR). To acquire CSIR, the transceivers have to leverage additional time slots and power for channel training in

practice [5]. In the contrary, another widely adopted intensity modulation, i.e., pulse position modulation (PPM) [6] does not need CSIR as it is not necessary for its receiver to determine the optimal detection threshold. Additionally, compared to OOK and M -PAM, PPM has much higher energy efficiency under the same average optical power. However, the detection of PPM is of higher implementation complexity as it requires accurate chip-level and symbol-level synchronization. To avoid using accurate system-level synchronization, Ghassemlooy *et al* proposed digital pulse interval modulation (DPIM) [7]. In DPIM, symbol duration is employed to modulate data. In this way, not only the implementation complexity is reduced, but also the transmission rate is improved as less chips are needed for each symbol in DPIM. Therefore, DPIM is considered more efficient than PPM [8], [9]. Recently, DPIM has been reported in the application of underwater OWC systems in [10] and [11].

The widely used detection method for DPIM is optimal threshold detection (OTD). Similarly as the threshold detection for OOK or M -PAM, OTD also requires the accurate CSIR to decide the optimal threshold. Besides, the detection method makes DPIM hampered by the error propagation. This is because that the symbol duration of each DPIM symbol is different, once a symbol error occurs, the whole packet is spoiled. This also explains why DPIM is often compared with other modulation schemes in packet error rate (PER) instead of bit error rate (BER) [1]. However, the comparison is unfair to the other modulation schemes. As the other modulation schemes are capable of combining with forward error correction (FEC) codes [12]–[15] for bit error correction which could lead to the great reduction of BER or PER, while to the best of our knowledge, there are no FEC codes that are able to correct the error propagation of DPIM caused by the bit position shift. Motivated by controlling its error propagation and facilitating its applications, especially the applications to combine with FEC, this paper proposes a new detection method for DPIM and a more robust transmission scheme.

Specifically, in this paper, we analyze the error propagation effect of DPIM and propose an ordered sequence detection (OSD). OSD can behave the error propagation by making the bit position shift bounded. It releases the requirement for the dynamic threshold determination and can considerably improve the system reliability. The proposed OSD detects a whole packet in a joint manner, with the knowledge of the number of chips L and the number of DPIM symbols N_s contained in a packet. Based on OSD, we propose a robust

digital pulse interval modulation (RPIM). The signal form of RPIM is very similar with that of DPIM. The difference lies in that power allocation is conducted among every K symbols of RPIM. In particular, the last of every K symbols is allocated with more power compared to the others to transmit information and simultaneously to provide a built-in synchronization signal. In this approach, the error propagation and the induced block error can be bounded in the K symbol slots with high probability. This enables combination with FEC code for further performance improvement. Aided by interleaver and FEC code, RPIM is much more reliable and robust than DPIM. In all context, we need to evaluate the performance improvement brought by OSD and RPIM, and determine the optimal K and optimal power allocation in RPIM scheme given L and N_s . These are all critical problems. By addressing these problems, the contributions of this paper are summarized as follows.

- The OSD is proposed for DPIM. The approximate uncoded BER of conventional DPIM with OTD and that with the proposed OSD are mathematically analyzed over additive white Gaussian (AWGN) channels in the high signal-to-noise ratio (SNR) regime.
- The RPIM is proposed. The approximate uncoded BER performance of RPIM with OSD is also analyzed. All analytical results hinge on order statistic theory and are validated by simulations. Although we analyze all systems over the simplest AWGN channels, the derived analytical results can be easily extended other optical wireless channels.
- The parameter optimization including finding optimal K and optimal power allocation for RPIM with OSD is probed. Specifically, as the expression of BER contains integral part, we propose a bisection algorithm based numerical optimization method to find the optimal power allocation for uncoded system. The optimization of parameter K is a discrete optimization problem and we study it via extensive search and by simulations. For the parameter optimization in coded system, we also rely on simulations.
- We make extensive comparisons among coded and uncoded DPIM with OTD, DPIM with OSD and RPIM with OSD over AWGN channels. To fully show the superiority of the proposed schemes, we also make comparisons over Gamma-Gamma turbulence channels. All comparison results demonstrate that the proposed RPIM and OSD outperform existing scheme greatly.

The remainder of the paper is organized as follows. The system model of DPIM with OSD and that of RPIM with OSD are introduced in Section II. Section III analyzes the error propagation effect of conventional DPIM with OTD, and shows how OSD and RPIM help behave the error propagation. In this section, we also mathematically derive the approximate uncoded BER performance of conventional DPIM with OTD, that of DPIM with OSD and that of RPIM with OSD over AWGN channels. Section IV validates the analysis by simulations, investigates the impact of parameter settings on performance and discusses the simulation results not only over

AWGN channels but also over Gamma-Gamma turbulence channels. Conclusions are drawn in the last section.

In this paper, following notations are employed. Vectors and matrices are represented by boldface letters. Scalars are denoted by the normal letters. $\mathbb{E}\{\cdot\}$ represents the expectation operation. $\text{sign}(x)$ stands for a sign function that extracts the sign of a real number.

II. SYSTEM MODEL

In this section, the system model of conventional DPIM with OSD will be firstly presented and then followed by the system model of the new RPIM with OSD. To address the concern of the detection complexity, the computational complexity analysis will also be included.

A. System Model of DPIM with OSD

Fig. 1 shows the system model of DPIM with OSD. In the depicted system model, M -ary DPIM is employed. We assume that there are L chips and N_s symbols in a packet. In other words, the signal form of DPIM is composed of N_s signal forms and the total length is L chips. Regarding the signal form of each symbol, there exist two categories including that with guard interval (GI) and that without. To demonstrate the differences, we show the signal forms of 4-DPIM without GI and that of 4-DPIM with 1 GI in Fig. 2. As shown in Fig. 2, data bits $\{00, 01, 10, 11\}$ are mapped the signal forms with intensity $\{A, A0, A00, A000\}$ if there is no GI and with intensity $\{A0, A00, A000, A0000\}$ if there is 1 GI, where A is the peak optical power. In this paper, we consider the general case where there are g ($g \in \mathbb{N}$) GIs, the average symbol duration can be written as

$$L_s = \frac{1}{M} \sum_{l=1}^M l + g = \frac{M + 2g + 1}{2}. \quad (1)$$

At the receiver, we assume that it is with accurate chip-level synchronization, accurate packet-level synchronization but without accurate symbol level synchronization. The received signal y of t -th chip can be written as

$$y(t) = hx(t) + n(t), \quad (2)$$

where h is the channel fading coefficient and remains constant during the transmission of a packet, $x(t)$ is the transmitted optical signal intensity (either 0 or A), and $n(t)$ is real-valued AWGN noise with zero mean and variance σ_n^2 . Without loss of generality, we assume $h = 1$ for the convenience of performance analysis. And it is noted that the analysis can be extend to other channels by considering the distribution of h , such as Gamma-Gamma turbulence channels for free space optical communications [16]–[18]. Due to the limitation of the paper length, we omit the analysis for these generalizations and only investigate them by simulations.

As shown in Fig. 1, the received signals of all L -chips are transformed into electrical signal by the photo-detector, stored in the buffer and denoted by $\mathbf{y} = [y(1), y(2), \dots, y(L)]$. A sorting algorithm is then performed to sort the entries of \mathbf{y} , which outputs the order index $i(t) \in \{1, 2, \dots, L\}$ of each

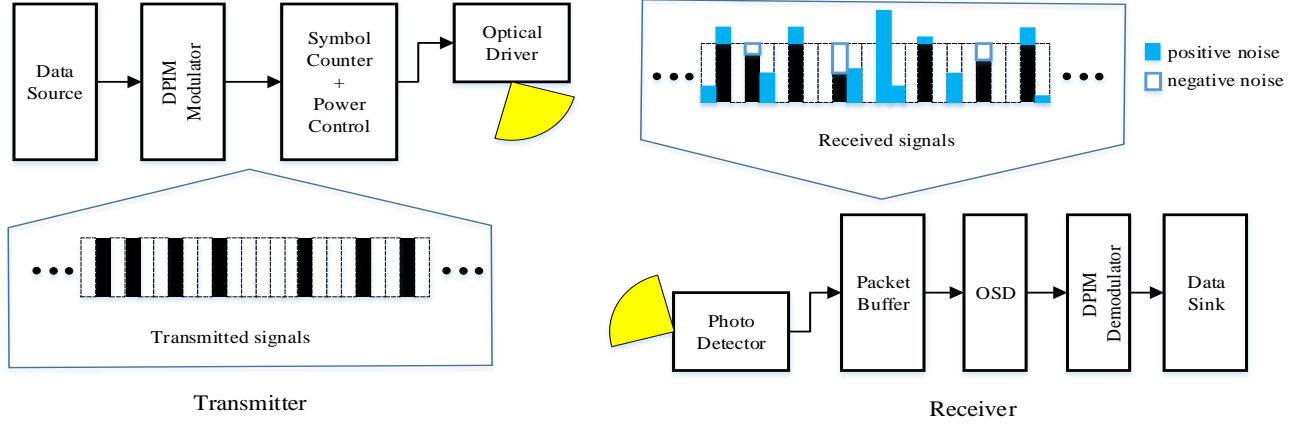


Fig. 1. System model block of DPIM with OSD

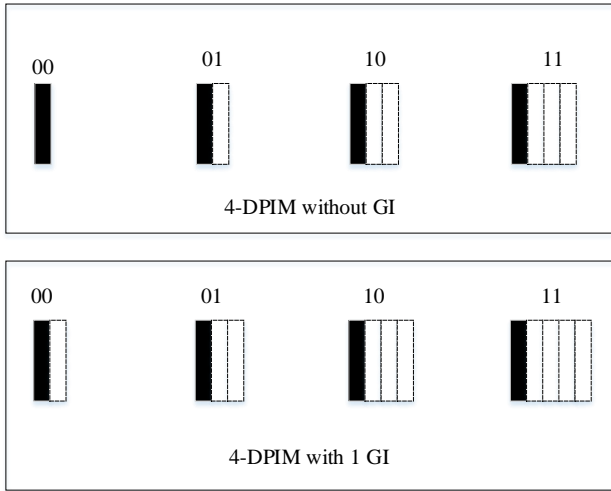


Fig. 2. The signal forms of DPIM

received signal. For the values of $i(t)$, if $i(1) = 3$, it means that $y(1)$ is the 3-th largest, if $i(2) = 100$, it means that $y(2)$ is 100-th largest and so on so forth. There are L chips in total. Therefore, $i(t)$ ranges from 1 to L for any t . After the values of $i(t)$ are determined, we then detect the N_s largest $y(t)$ as A and the others as 0. Mathematically, the detected signal sequence can be written as

$$d(t) = \begin{cases} A, & 1 \leq i(t) \leq N_s, \\ 0, & N_s + 1 \leq i(t) \leq L. \end{cases} \quad (3)$$

Then by inputting $d(t)$ into conventional DPIM demodulator, we finally get the data bits.

B. System Model of RPIM with OSD

To enhance the system reliability, a robust scheme, called RPIM, is proposed. As aforementioned in Section I, the signal form of RPIM is similar as that of DPIM. As illustrated in Fig. 3, the power for sending the last of every K symbols is A_H and the power for sending the other symbols is A_L in RPIM. As the symbols with power A_H not only carry information but also offer a built-in synchronization signal, while the other symbols with power A_L only carry information, we set A_H greater than A_L . With such specific power allocation, the transmit signal $x(t)$ in (2) could be 0, A_L or A_H . For simplicity, we hypothesis that the number of symbols N_s in a packet can be divided by K , which means N_s can be expressed as $N_s = KQ$ and Q is a positive integer. For fair comparison with DPIM under the same power constraint, the power allocation in every K symbols of RPIM should satisfy

$$(K - 1)A_L + A_H = KA. \quad (4)$$

At the receiver, the clipped received signal vector \mathbf{y} is also stored and operated by a sorting algorithm to sort the entries and to get the order index $i(t)$. Then in the first detection phase, the Q largest of $y(t)$ are detected as A_H , the indices of which is recorded as t_1, t_2, \dots, t_Q . We then sort those indices in an ascent order $t'_1 < t'_2 < \dots < t'_Q$ and set $t'_0 = 0$. After that, by sorting vector $\mathbf{y}(t'_i + 1 : t'_{i+1} - 1)$, the $(K - 1)$ largest values of which are detected as A_L and others as 0 for any $i = 0, 1, \dots, Q - 1$, we rebuild the transmitted signals. Hereafter, we refer the detection of A_L as the second detection phase. Moreover, as there are $K - 1$ symbols in the signal vector $\mathbf{y}(t'_i + 1 : t'_{i+1} - 1)$, if $t'_{i+1} - t'_i < K(g + 1)$, zeros will be embedded such that $K - 1$ symbols can be detected. At last, by inputting the signal into conventional DPIM demodulator, we finally obtain the data bits. The detailed OSD algorithm for RPIM is listed in Algorithm 1.

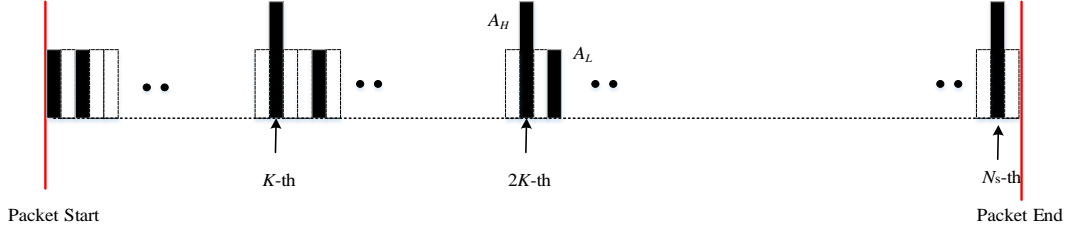


Fig. 3. The signal forms and sequence structure of RPIM

Algorithm 1 OSD Algorithm for RPIM

Input: \mathbf{y} , L , N_s and Q
Sort \mathbf{y} and output the order index $i(t)$.
Detect $1 \leq i(t) \leq Q$ as A_H and output the indices t_1, t_2, \dots, t_Q .
Sort t_1, t_2, \dots, t_Q in an ascent order $t'_1 < t'_2 < \dots < t'_Q$.
 $t_0 = 0$.
for $i = 0 : Q - 1$ **do**
 if $t'_{i+1} - t'_i < K$ **then**
 Embed zeros.
 end if
 Sort $\mathbf{y}(t'_i + 1 : t'_{i+1} - 1)$ and detect the $(K - 1)$ largest as A_L and others as 0.
end for

C. Computational Complexity Analysis

The complexity of OSD to detect DPIM is that of the sorting algorithm performing on L received signals. The complexity is at most $O(L^2)$. This complexity can be reduced using advanced sorting algorithm. As the complexity is acceptable and those low-complexity sorting algorithms are beyond the scope of this paper, we overlook the case when advanced sorting algorithms are used.

The complexity of OSD to detect RPIM is that of the two detection phases. The first involves a sorting algorithm operating on L received signals. As analyzed, the complexity is at most $O(L^2)$. The second involves sorting algorithms operating on $\mathbf{y}(t'_i + 1 : t'_{i+1} - 1)$ for all $i = 0, 1, \dots, Q - 1$. The average length of $\mathbf{y}(t'_i + 1 : t'_{i+1} - 1)$ is around L/Q and the sorting operations are conducted for Q times. Thus, the complexity of the second detection phase is around $O(L^2/Q)$. In summary, the total complexity of two detection phases is also around $O(L^2)$ and totally acceptable.

III. ERROR PROPAGATION EFFECT AND BER ANALYSIS IN HIGH SNR REGIME

This section will present how error propagation effect damages the BER performance of conventional DPIM with OTD and how the proposed OSD and RPIM with OSD help behave the error propagation. In this part, we will also mathematically derive the approximate uncoded BER performance of conventional DPIM with OTD, that of DPIM with OSD and that of RPIM with OSD over AWGN channels based on order statistic theory.

A. Error Propagation Effect and BER Analysis of Conventional DPIM With OTD

For conventional DPIM with OTD, the chip error probability can be expressed as

$$P_c = P(0)P(0 \rightarrow A) + P(A)P(A \rightarrow 0), \quad (5)$$

where $P(0)$, $P(A)$ represent the probabilities of sending 0 and A , respectively and $P(0 \rightarrow A)$, $P(A \rightarrow 0)$ represent the error detection probabilities. Conditioned that the optimal threshold is A_T , the chip error probability can be expressed as

$$P_c = P(0) \int_{A_T}^{\infty} \frac{1}{\sqrt{2\pi}\sigma_n} e^{-\frac{x^2}{2\sigma_n^2}} dx + P(A) \int_{-\infty}^{A_T} \frac{1}{\sqrt{2\pi}\sigma_n} e^{-\frac{(A-x)^2}{2\sigma_n^2}} dx. \quad (6)$$

By taking the first derivative of P_c with respect to A_T , we have

$$\frac{\partial P_c}{\partial A_T} = P(A) \frac{1}{\sqrt{2\pi}\sigma_n} e^{-\frac{(A-A_T)^2}{2\sigma_n^2}} - P(0) \frac{1}{\sqrt{2\pi}\sigma_n} e^{-\frac{A_T^2}{2\sigma_n^2}} \quad (7)$$

By reformulating and solving the equation $\frac{\partial P_c}{\partial A_T} = 0$, we get

$$(A - A_T)^2 = A_T^2 + 2\sigma_n^2 \ln \frac{P(A)}{P(0)}. \quad (8)$$

Thus, the optimal threshold A_T is derived as

$$A_T = \frac{A}{2} - \frac{\sigma_n^2}{A} \ln \frac{P(A)}{P(0)}. \quad (9)$$

In DPIM, $P(A) = 1/L_s$ and $P(0) = 1 - 1/L_s$. Substituting them into (9), we get

$$A_T = \frac{A}{2} + \frac{\sigma_n^2}{A} \ln (L_s - 1). \quad (10)$$

Summarizing all above, the chip error probability P_c can be calculated by

$$P_c = \frac{L_s - 1}{L_s} Q \left(\frac{A}{2\sigma_n} + \frac{\sigma_n}{A} \ln (L_s - 1) \right) + \frac{1}{L_s} Q \left(\frac{A}{2\sigma_n} - \frac{\sigma_n}{A} \ln (L_s - 1) \right). \quad (11)$$

where $Q(\cdot)$ is the Gaussian Q function.

Here, we only consider the case that there is one chip error in a wrongly detected packet. This is reasonable because the chip error detection occurs with a very low probability especially in high SNR regime such that the case with one chip

error dominates all other error cases. Based on this assumption, we have the following proposition

Proposition 1: In high SNR regime, the BER of DPIM with OTD can be approximated as

$$P_{e1} \approx \sum_{t=1}^L \frac{N_s - \mathcal{N}(t)}{2N_s} P_c (1 - P_c)^{L-1} \quad (12)$$

where $\mathcal{N}(t)$ stands for the number of symbols (i.e., the number of A s) between the first chip and the t -th chip. Based on the approximation $\mathbb{E}\{\mathcal{N}(t)\} \approx t/L_s$, the BER of DPIM with OTD can be derived as

$$P_{e1} \approx \frac{L-1}{4} P_c (1 - P_c)^{L-1}. \quad (13)$$

Proof: For any possible chip error, there exist only two events. The first is that 0 is wrongly detected as A , which is called *false alarm error*. In this event, additional $\log_2 M$ bits are embedded into the sequence. Consequently, all the sequel information bits are shifted right by $\log_2 M$ bits and the total number of bits also increases. As a result, all information bits from the *false alarm error* to the end of bit sequence are like random guess (i.e., with correct detection probability being $1/2$). The second is that A is detected as 0, which is called *erasure error*. In this event, a symbol is missed and $\log_2 M$ bits are removed from the sequence. Consequently, all the sequel information bits are shifted left by $\log_2 M$ bits and the total number of bits decreases. As a result, all information bits from the *erasure error* to the end of bit sequence are also like random guess. Summarizing all above, in both events, the number of error bits equals $[N_s - \mathcal{N}(t)] \log_2 M/2$ like random guess. It is noted that the current chip detection error may also influence the detection of a former symbol. As the influence on BER is too small compared to the error propagation effect, we omit the fact. Based on above analysis, considering the total number of bits is $N_s \log_2 M$, the BER of DPIM can be derived as Proposition 1 states. ■

B. Error Propagation Effect and BER Analysis of Conventional DPIM with OSD

Above analysis in the proof of Proposition 1 shows that one chip error (either a *false alarm error* or an *erasure error*) in OTD will spoil the detection of bit sequence from the chip where error happens to the end of the sequence. Different from OTD resulting into independent chip errors, OSD imposes a constraint on the errors that the number of *false alarm errors* is the same as the number of *erasure errors*. This is because the number of detected A s is N_s , as same as that in the transmit signals. This indicates that as long as a *false alarm error* (or an *erasure error*) occurs, it is accompanied with an *erasure error* (or a *false alarm error*). Here similarly, we assume that there is only one pair of errors, i.e., a *false alarm error* associated with an *erasure error*, in a wrongly detected packet by OSD. The probability of error detection can be expressed as

$$P_{0A} = \text{Prop}\{X_{0,1} > X_{A,N_s}\}, \quad (14)$$

where $X_{0,l}$ denotes the l -th largest received signal when 0 is transmitted and $X_{A,l}$ denotes the l -th largest received signal

when A is transmitted. P_{0A} in (14) is the probability that the largest received signal of transmitting 0 is wrongly detected as A , meanwhile the smallest received signal of transmitting A is wrongly detected as 0. Based on order statistic theory, the following lemma can be derived.

Lemma 1: The probability of error detection for DPIM with OSD can be derived as

$$P_{0A} = \mathcal{OR}(0, A, N - N_s, N_s, \sigma_n) \quad (15)$$

where $\mathcal{OR}(\mu_1, \mu_2, n_1, n_2, \sigma_n)$ is an order statistic function defined as

$$\mathcal{OR}(\mu_1, \mu_2, n_1, n_2, \sigma_n) = \int_{-\infty}^{+\infty} [1 - F_X(y, \mu_1, n_1)] f_Y(y, \mu_2, n_2) dy, \quad (16)$$

where

$$F_X(y, \mu_1, n_1, \sigma_n) = \frac{1}{2^{n_1}} \left[1 + \text{erf} \left(\frac{y - \mu_1}{\sqrt{2}\sigma_n} \right) \right]^{n_1}, \quad (17)$$

and

$$f_Y(y, \mu_2, n_2, \sigma_n) = \frac{n_2}{2^{n_2-1} \sqrt{2\pi}\sigma_n} \left[1 - \text{erf} \left(\frac{y - \mu_2}{\sqrt{2}\sigma_n} \right) \right]^{n_2-1} e^{-\frac{(y-\mu_2)^2}{2\sigma_n^2}}. \quad (18)$$

The proof of Lemma 1 can be found in Appendix A. Based on the derived expression of P_{0A} in Lemma 1, we have the following theorem.

Theorem 1: The BER of DPIM with OSD can be approximated as

$$P_{e2} \approx \sum_{t_1=1}^L \sum_{t_2=t_1+1}^L \frac{\mathcal{N}(t_2) - \mathcal{N}(t_1)}{L(L-1)N_s} P_{0A} \quad (19)$$

Considering the approximations $\mathbb{E}\{\mathcal{N}(t_2)\} \approx t_2/L_s$ and $\mathbb{E}\{\mathcal{N}(t_1)\} \approx t_1/L_s$, the BER of DPIM with OSD can be approximated as

$$P_{e2} \approx \frac{2L^2 - 7L + 5}{12L^2} P_{0A}. \quad (20)$$

Proof: A pair of errors will lead to the error propagation between the first error to the second error. Consequently, $[\mathcal{N}(t_2) - \mathcal{N}(t_1)] \log_2 M/2$ bit errors will occur like random guess. The probability of any (t_1, t_2) , $t_2 > t_1$ being pairwisely detected is $2/[L(L-1)]$. Summarizing above, Theorem 1 can be proved. ■

C. Error Propagation Effect and BER Analysis of Conventional RPIM with OSD

Based on the above analysis, it is found that OSD can help behave the error propagation by making the error detection bounded between the pair errors. To further improve the performance, a RPIM is proposed and more power (A_H) is used to transmit the last of every K -th symbol. Due to the property of OSD, we have the constraints for RPIM

$$P(A_L \rightarrow A_H) + P(0 \rightarrow A_H) = P(A_H \rightarrow A_L) + P(A_H \rightarrow 0), \quad (21)$$

and

$$P(A_L \rightarrow 0) + P(A_H \rightarrow 0) = P(0 \rightarrow A_H) + P(0 \rightarrow A_L). \quad (22)$$

Since $P(0 \rightarrow A_H)$ and $P(A_H \rightarrow 0)$ are much smaller than $P(A_L \rightarrow A_H)$ and $P(A_H \rightarrow A_L)$, we have

$$P(A_L \rightarrow A_H) \approx P(A_H \rightarrow A_L). \quad (23)$$

Similarly, as $P(0 \rightarrow A_H)$ and $P(A_H \rightarrow 0)$ are much smaller than $P(0 \rightarrow A_L)$ and $P(A_L \rightarrow 0)$, we have

$$P(0 \rightarrow A_L) \approx P(A_L \rightarrow 0). \quad (24)$$

Here, we also only consider the case there are a pair of errors either in the first phase of detecting A_H or in the second phase of detecting A_L . The error detection probability in the first phase of detecting A_H can be expressed as

$$P_{LH} = \text{Prop}\{X_{A_L,1} > X_{A_H,Q}\}. \quad (25)$$

and the error detection probability in the second phase of detecting A_L can be expressed as

$$P_{0L} = \text{Prop}\{X_{0,1} > X_{A_L,K-1}\}, \quad (26)$$

respectively. Based on Lemma 1, we have the the following corollary.

Corollary 1: P_{LH} and P_{0L} can be calculated as

$$P_{LH} \approx \mathcal{OR}(A_L, A_H, N_s - Q, Q, \sigma_n) \quad (27)$$

and

$$P_{0L} \approx \mathcal{OR}(0, A_L, KL_s - 1, K - 1, \sigma_n) \quad (28)$$

respectively.

According to Corollary 1, we can derive the following theorem.

Theorem 2: The BER of RPIM with OSD can be expressed as

$$P_{e3} \approx \sum_{t_1=1}^{N_s} \sum_{t_2=t_1+1}^{N_s} \frac{t_2 - t_1}{N_s(N_s - 1)N_s} P_{LH} + \sum_{t_1=1}^W \sum_{t_2=t_1+1}^W \frac{\mathcal{N}(t_2) - \mathcal{N}(t_1)}{W(W-1)(K-1)} (1 - P_{LH}) P_{0L}, \quad (29)$$

where

$$W = KL_s - 1, \quad (30)$$

where W represents the average number of chips in the second phase of detection. Using the approximation $\mathcal{N}(t) = t/L_s$, the BER of RPIM with OSD can be approximated as

$$P_{e3} \approx \frac{2N_s^2 - 7N_s + 5}{12N_s^2} P_{LH} + \frac{2W^2 - 7W + 5}{12W(K-1)L_s} (1 - P_{LH}) P_{0L}. \quad (31)$$

The proof of Theorem 2 can be found in Appendix B.

IV. OPTIMAL POWER ALLOCATION FOR UNCODED RPIM WITH OSD

The parameter settings determine the system performance. The parameters include K , A_L and A_H . As K is a discrete variable, it can be optimized by exhaustive search and the complexity is acceptable since the optimization is done off-line. Thus, this part will only discuss the optimization of the continuous variable optimization of A_L and A_H given a fixed K symbol duration in uncoded systems. This is a typical power allocation problem and can be formulated as

$$A_L^*, A_H^* = \arg \min_{A_L, A_H} P_{e3}(A_L, A_H) \quad (32)$$

subject to : $0 < A_L < A_H$ and (4).

By reformulating (4), we can get

$$A_H = KA - (K-1)A_L. \quad (33)$$

By substituting A_H into (31), we get

$$P_{e3}(A_L) = UP_{LH}(A_L) + V[1 - P_{LH}(A_L)]P_{0L}(A_L). \quad (34)$$

where U and V are constants and defined by

$$U = \frac{2N_s^2 - 7N_s + 5}{12N_s^2}, \quad (35)$$

and

$$V = \frac{2W^2 - 7W + 5}{12W(K-1)L_s}. \quad (36)$$

As $P_{e3}(A_L)$ in (34) is complex, here we use the upper bound for its optimization, which is defined as

$$P_{e3}^{\text{up}}(A_L) = UP_{LH}(A_L) + VP_{0L}(A_L). \quad (37)$$

It is an upper bound because the term $1 - P_{LH}(A_L)$ in (34) is less than or equal to 1. By taking the first derivative of (37) with respect to A_L , we can get

$$f(A_L) \triangleq \frac{dP_{e3}(A_L)}{dA_L} = U \frac{dP_{LH}(A_L)}{dA_L} + V \frac{dP_{0L}(A_L)}{dA_L} \quad (38)$$

Due to the complex integral part in the $\mathcal{OR}(\cdot)$ function in (16), the closed-form solution of the equation $f(A_L) = 0$ is difficult to obtain. Thus, we attempt to get the solution by using a bisection algorithm listed in Algorithm 2.

In the following, we seek to show that the simple bisection algorithm is effective for solving the optimal power allocation problem in uncoded RPIM systems with OSD. We set the number of symbols $N_s = 1000$ and do power allocation in every $K = 10$ symbols. We set other parameters as follows. the SNR $\gamma = A^2/\sigma^2 = 15, 17$ dB, the modulation order $M = 4$, the number of guard intervals $g = 1$, algorithm parameter tolerance $\tau = 1e-3$ and maximum iteration $N_{\text{max}} = 1000$. Fig. 4 shows the variation of A_L as the iteration number increases. Result shows that the algorithm converges very fast and it takes 10 iterations to converge. We also show the variation of P_{e3} in (37) during the iteration process in Fig. 5. Fig. 5 demonstrates that the bisection algorithm approaches the optimal power allocation easily. Fig. 5 also demonstrates that the power allocation affects the BER performance greatly and a small shift of A_L from the optimal point will lead to 1 or 2 orders increases of BER. This study verifies the effectiveness

TABLE I
OPTIMAL POWER ALLOCATION A_L/A_H FOR $N_s = 100$ AND $N_s = 1000$ WHEN $\gamma = 15, 17$ dB.

-	$K = 5$	$K = 10$	$K = 20$	$K = 25$	$K = 50$
$N_s = 100, \gamma = 15$ dB	0.774A/1.904A	0.887A/2.017A	0.945A/2.045A	0.957A/2.032A	0.979A/2.029A
$N_s = 100, \gamma = 17$ dB	0.795A/1.820A	0.895A/1.945A	0.948A/1.988A	0.959A/1.984A	0.980A/1.980A
$N_s = 1000, \gamma = 15$ dB	0.732A/2.072A	0.865A/2.215A	0.933A/2.273A	0.947A/2.272A	0.974A/2.274A
$N_s = 1000, \gamma = 17$ dB	0.766A/1.936A	0.880A/2.080A	0.940A/2.140A	0.952A/2.152A	0.977A/2.127A

Algorithm 2 Bisection Algorithm for Power Allocation

Input: L, K, A, M, g, σ_n , tolerance τ and maximum iteration N_{\max}

Output: A_L and A_H

Initiation: $a = 0$ and $b = A$

$N_{\text{iter}} = 1$

while $N_{\text{iter}} \leq N_{\max}$ **do**

$c = \frac{a+b}{2}$

if $f(c) = 0$ or $(b - a)/2 < \tau$ **then**

$A_L = c$ and $A_H = KA - (K - 1)A_L$

Stop

end if

$N_{\text{iter}} = N_{\text{iter}} + 1$

if $\text{sign}(f(c)) = \text{sign}(f(a))$ **then**

$a = c$

else

$b = c$

end if

end while

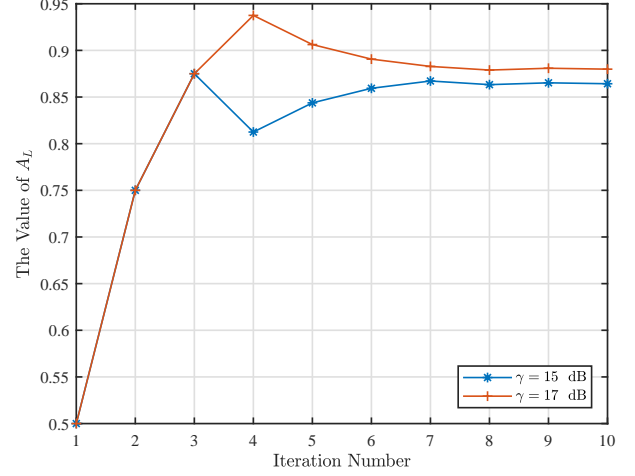


Fig. 4. The value of A_L as the iteration number increases

of the bisection algorithm in solving the problem with fast converge speed, good performance and low complexity. Using the bisection algorithm listed in Algorithm 2, we get several optimal power allocation results including A_L and A_H for system configurations $N_s = 100$ and $N_s = 1000$ as listed in Table I when $\gamma = 15$ and 17 dB. Results in Table I show that for different N_s setups, the optimal A_L s vary in a small range and sometimes are the same in uncoded system. For different K s, A_L is small when K is small and larger as K becomes larger. A_L increases very slowly and approaches A . In the following simulations of uncoded systems, without otherwise noted, we will use these results for power allocation.

V. SIMULATION AND DISCUSSION

This section will present the simulation results. We divide it into three subsections. In the first subsection, we will validate the approximate performance analysis results given in Proposition 1, Theorem 1 and Theorem 2. In the second subsection, we will study the impact of the parameter setups on the system performance of the proposed RPIM with OSD. In the last subsection, we will extensively compare three schemes over AWGN channels and over Gamma-Gamma turbulence channels.

A. Validation of Analysis

In this subsection, we validate the approximate performance analysis of conventional DPIM with OTD (i.e., Proposition 1),

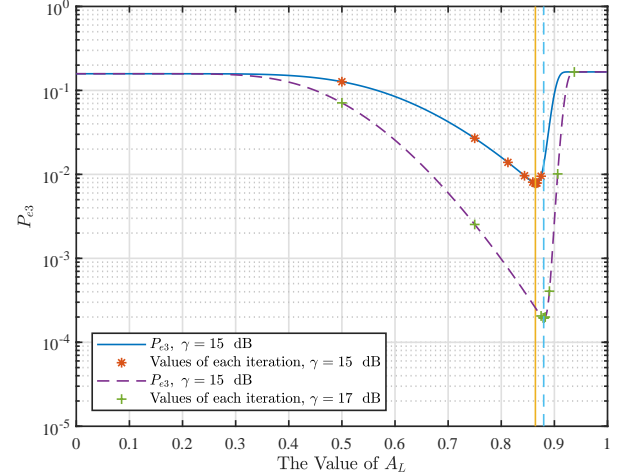


Fig. 5. The approximate BER performance P_e versus the value of A_L when $N_s = 1000$, $\gamma = 15$ and 17 dB.

that of conventional DPIM with OSD (i.e., Theorem 1) and that of the proposed RPIM with OSD (i.e., Theorem 2), in Figs. 6, 7 and 8, respectively.

In detail, Fig. 6 shows the simulated and approximate BER performance of conventional DPIM with OTD versus SNR ranging from 10 dB to 24 dB. Two cases with the number of symbols in a packet $N_s = 100$ and 1000 are considered. For both cases, analytical results agree well with the simulation results in high SNR regime. Specifically, when $N_s = 100$,

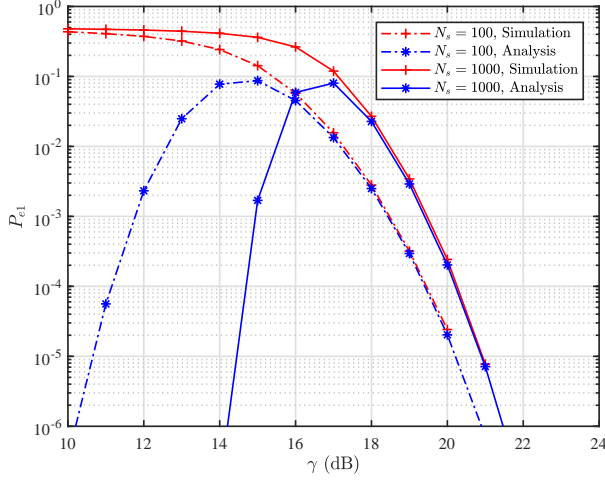


Fig. 6. The simulated and approximate BER performance conventional DPIM with OTD.

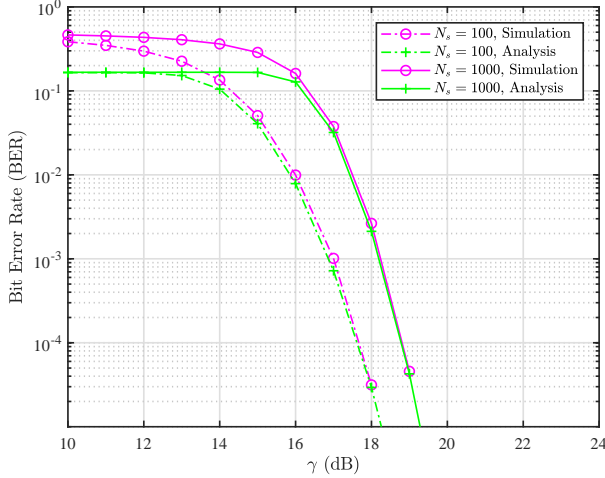


Fig. 7. The simulated and approximate BER performance of conventional DPIM with OSD.

analysis result is close to the real BER if $\gamma > 16$ dB. When $N_s = 1000$, analysis result is close to the real BER if $\gamma > 17$ dB. Both cases are as what Proposition 1 states.

Fig. 7 shows the simulated and approximate BER performance of the conventional DPIM with OSD. The analytical result is that given by Theorem 1. Similarly, two cases with the number of symbols in a packet $N_s = 100$ and $N_s = 1000$ are considered. For either cases, analytical result in Theorem 1 approximates to the simulation results in high SNR regime. For $N_s = 100$, the SNR where they agree well is greater than 14 dB. For $N_s = 1000$, the SNR where they agree well is greater than 16 dB. Thus, results in this figure validate Theorem 1.

Fig. 8 shows the simulated and approximate BER performance of the proposed RPIM with OSD where $K = 10$. We also consider two cases with the number of symbols in a packet $N_s = 100$ and $N_s = 1000$. One can also easily draw the conclusion that analytical results given in Theorem 2 agree

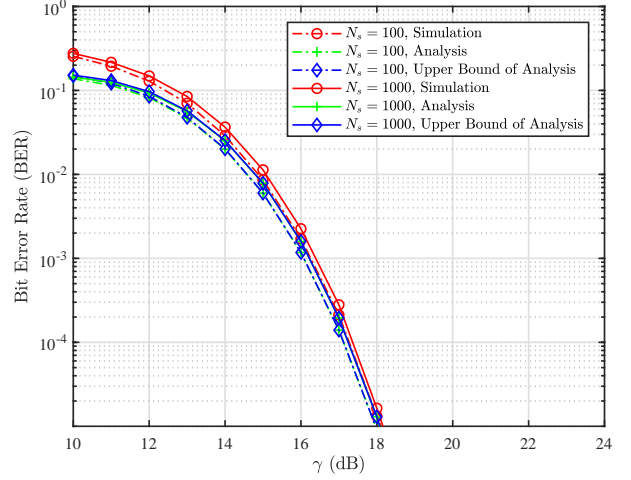


Fig. 8. The simulated and approximate BER performance of conventional RPIM with OSD, where $K = 10$.

well with the simulated BER results in high SNR regime. For $N_s = 100$ and $N_s = 1000$, the BER are almost the same and the SNR threshold where simulation and analysis agree well is 13 dB. The fact that same performance are achieved for different N_s in uncoded system can be explained because no matter how many symbols it has in a packet, the block error is bounded in every $K = 10$ symbol duration. This is different from DPIM shown in Figs. 6 and 7 because error propagation can not be precisely under control in DPIM either with OTD or with OSD. In Fig. 8, we also illustrate the upper bound of the approximate BER performance in (37). It is shown that the upper bound of BER approximation is pretty tight in the depicted SNR regime. This indicates that we are correct to use the upper bound of the BER approximation in the bisection search algorithm for optimal power allocation. The upper bound can be calculated with low complexity, which makes the bisection search algorithm computationally efficient.

B. Impact of Different Parameter Settings on the Performance of RPIM with OSD

In Section IV, we have discussed the impact of power allocation (parameters A_L and A_H) on the uncoded RPIM system performance. In this subsection, we will investigate how the parameter K affects the system reliability. Moreover, as extant communication systems are almost all coded, we also investigate how parameter K and power allocation (parameters A_L and A_H) affect coded BER by simulations in this subsection. In coded system, we adopt an interleaver of length $K \log_2 M$, a convolution code with $1/2$ code rate and a Viterbi hard decoder.

Firstly, we compare the BER performance of uncoded RPIM with OSD systems with different K s. The parameter $N_s = 100$ and $\gamma = 15$ dB. As N_s can be divided by K , we simulate cases that $K = \{5, 10, 20, 25, 50\}$. The other parameters including A_L and A_H are set according to the Table I. The results are illustrated in Fig. 9. Fig. 9 shows the variation of BER performance along with the increase of K . As one can

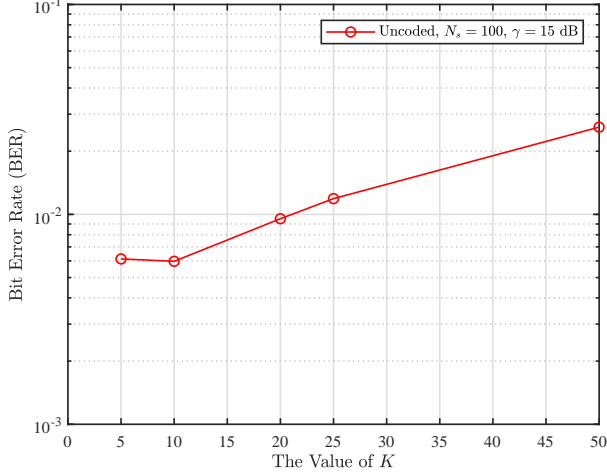


Fig. 9. The BER performance of uncoded RPIM with OSD along with the increase of K where $N_s = 100$ and $\gamma = 15$ dB.

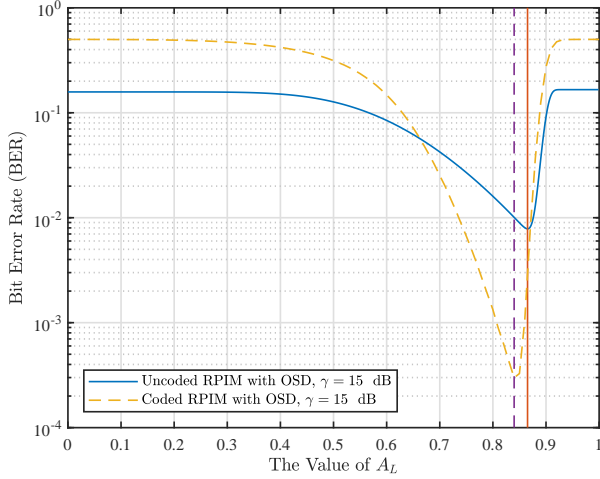


Fig. 10. The BER performance of RPIM with OSD versus the value of A_L .

observe, the optimal K in this system is 10. For $K > 10$, the performance degrades as K increases. This is because bit error propagates in a wider range for larger K . It also demonstrates that even though K affects the uncoded system performance, the impact is not so considerable. The BER ranges within one order from $6e-3$ to $2.5e-2$ as K varies.

Secondly, we probe how power allocation factors (i.e., A_L and A_H) affect the BER performance in coded system. As A_L and A_H are coupled, we only show the uncoded BER performance versus the value of A_L in Fig. 10. Results show that the power allocation affects the BER performance of coded system a lot. For comparison purpose, we also illustrate the BER performance of uncoded systems versus the value of A_L . One can observe that the optimal power allocation in coded system are different that in uncoded system. More specifically, the power for the last of every K symbols A_H in coded system are greater than that in uncoded system. This can be explained as follows. Increasing A_H and reducing A_L will

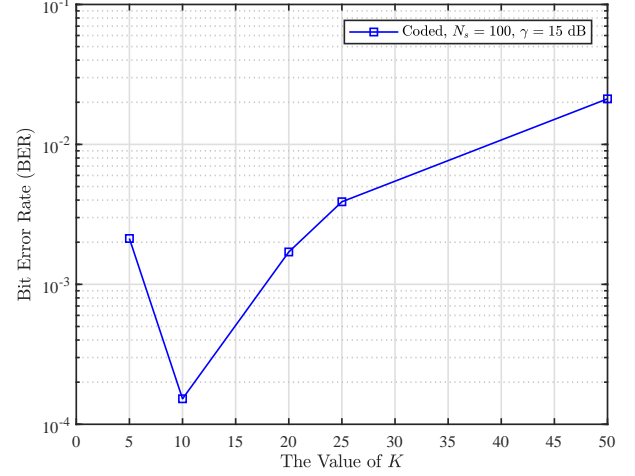


Fig. 11. The variation of uncoded BER performance along with the increase of K when $N_s = 100$ and $\gamma = 15$ dB.

reduce the BER of the first detection phase and increase the BER of the second detection phase. And aided by interleaver and FEC code, the bit errors of the second phase can be corrected. Thus, in coded system, the optimal power allocation for the last of every K symbols is larger. But it should not be too large because too large A_H will lead to too many errors in the second detection phase, which could be beyond the correction capability of the employed FEC code.

Thirdly, we investigate how parameter K affects the BER performance of coded RPIM with OSD. Similarly, we set $N_s = 100$ and the alternative K 's are $\{5, 10, 20, 25, 50\}$. The simulation results are given in Fig. 11. Results show that K is very important in coded systems. The reason is as follows. error propagation of RPIM with OSD will be bounded in K symbol duration. In other words, the parameter K decides the length of error propagation and thus determines whether the interleaver and FEC could be able to correct the error bits. In this simulated system, the optimal K is also 10. Changing K results into a larger BER variation from $1.5e-4$ to $2e-2$ in coded system than that in uncoded system shown in Fig. 9.

C. Extensive Comparisons over AWGN Channels and over Gamma-Gamma Turbulence Channels

We compare uncoded and coded BER of DPIM with OTD, DPIM with OSD and RPIM with OSD over two kinds of channels. The first kind is AWGN channels. This is the simplest but the basic channel model. The other kind is Gamma-Gamma strong turbulence channels. This is because both DPIM and RPIM belong to the high energy-efficiency modulation family and widely applied in outdoor OWC including free space optical communications and underwater OWC. Gamma-Gamma turbulence channels is one of widely investigated FSO channel models. Here we take it as an example to verify the extension of our proposed schemes. In all simulations, $N_s = 1000$ and $K = 100$. Optimal power allocation is obtained by exhaustive search and considered for RPIM with OSD. In coded system as that in Section V-B, an interleaver of length $K \log_2 M$ and

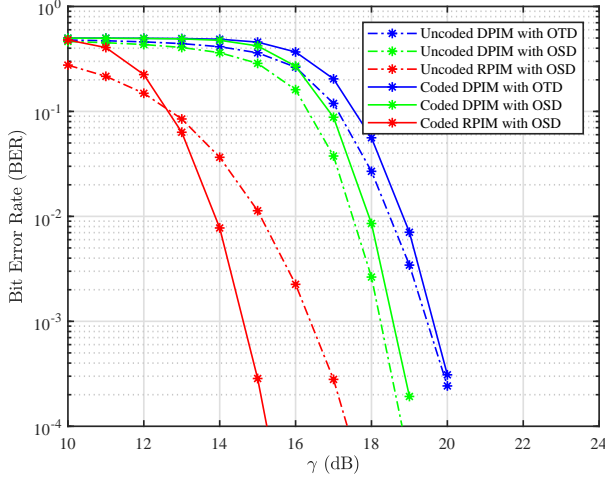


Fig. 12. The performance comparison among DPIM with OTD, DPIM with OSD and RPIM with OSD over AWGN channels, where $N_s = 1000$ and $K = 10$.

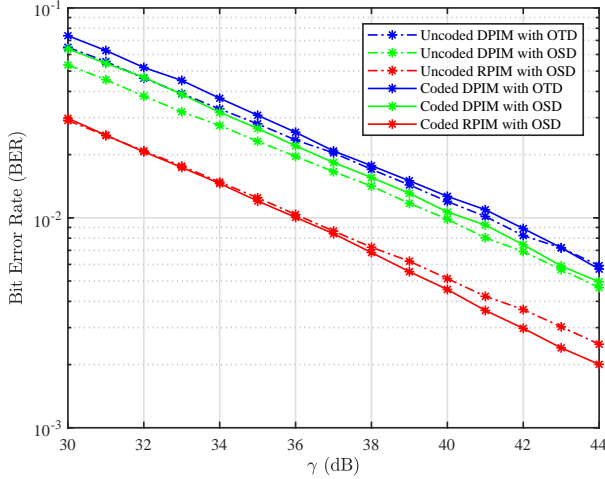


Fig. 13. The performance comparison among DPIM with OTD, DPIM with OSD and RPIM with OSD over Gamma-Gamma turbulence channels, where $N_s = 1000$ and $K = 10$.

a simple convolution code with 1/2 code rate are adopted. In Gamma-Gamma channels, the average channel gain is set to be 0 dB.

Fig.12 shows the comparison results over AWGN channels. Results demonstrate that the proposed RPIM and OSD greatly outperforms conventional schemes in either coded and uncoded systems. Specifically, RPIM with OSD outperforms DPIM with OTD and DPIM with OSD by around 3 dB and 2 dB in uncoded systems, respectively; the gain becomes much larger and are around 5 dB and 4 dB in coded systems respectively. Results also demonstrate that the FEC code can help RPIM with OSD to improve system performance, while it can not help and even degrades the performance of DPIM with OTD and that of DPIM with OSD. This indicates that our proposed RPIM with OSD enables the combination with FEC codes, which can provide additional coding gain. The DPIM

either with OTD or with OSD has even worse performance if combined with FEC because the length of their error propagation is too long, which results into the burst bit errors that can not be corrected.

Fig. 13 shows the comparison results over Gamma-Gamma turbulence channels. Note that for DPIM with OSD and RPIM with OSD and power allocation over Gamma-Gamma turbulence channels, no instantaneous CSIR is required, while for DPIM with OTD, instantaneous CSIR is a must. In Gamma-Gamma turbulence channels, the BER performance of all schemes is dominated by the most severe fading. Even through it has relative large average SNR of channels, its performance is still very limited. To observe the performance well, we simulate the system in higher SNR regime ranging from 30 dB to 44 dB. Simulation results in Fig. 13 exhibit similarly as that in AWGN channels. We similarly conclude that the proposed RPIM with OSD can bring considerable gain over Gamma-Gamma turbulence channels. For better performance over such channels, other techniques such as hybrid automatic repeat request (ARQ) [19], [20] can be jointly adopted to provision users quality-of-service (QoS).

Finally, we note that the proposed detection method and transmission scheme are not affected by ambient noise. In addition, the applications of the proposed detection method and transmission scheme are not limited in OWC and can be extended to address the error propagation problem of other modulation schemes similar as DPIM.

VI. CONCLUSION

This paper proposed an OSD for DPIM and a more reliable RPIM with OSD. With a bit increase of detection complexity from $\mathcal{O}(L)$ to the order of $\mathcal{O}(L^2)$, OSD considerably improves the system performance in terms of BER. Through specific power allocation, RPIM makes the error propagation bounded and enables the combination with FEC to greatly improve the system reliability. The approximate uncoded BER performance of three schemes including DPIM with OTD, DPIM with OSD and RPIM with OSD was derived and we verified all the analysis by simulations. They agreed very well in high SNR regime. We studied how parameter settings affect the performance by simulations. We compared three schemes over AWGN channel and over Gamma-Gamma turbulence channels. We conclude that the RPIM with OSD can bring considerable performance gain and enhance the system reliability significantly.

APPENDIX A PROOF OF LEMMA 1

For the order statistics $X_{0,1}, X_{0,2}, \dots, X_{0,L-N_s}$,

$$X_{0,1} > X_{0,2} > \dots > X_{0,L-N_s}, \quad (39)$$

and the probability density function (PDF) [21] of $X_{0,1}$ can be expressed as

$$f_{X_{0,1}}(x) = (L - N_s) [F_0(x)]^{L-N_s-1} f_0(x), \quad (40)$$

and the cumulative density function (CDF) of $X_{0,1}$ can be expressed as

$$F_{X_{0,1}}(x) = [F_0(x)]^{L-N_s}, \quad (41)$$

where

$$f_0(x) = \frac{1}{\sqrt{2\pi}\sigma_n} e^{-\frac{x^2}{2\sigma_n^2}}, \quad (42)$$

and

$$F_0(x) = \frac{1}{2} \left[1 + \operatorname{erf} \left(\frac{x}{\sqrt{2}\sigma_n} \right) \right]. \quad (43)$$

For the order statistics $X_{A,1}, X_{A,2}, \dots, X_{A,N_s}$,

$$X_{A,1} > X_{A,2} > \dots > X_{A,N_s}, \quad (44)$$

and the PDF of X_{A,N_s} can be expressed as

$$f_{X_{A,N_s}}(x) = N_s [1 - F_A(x)]^{N_s-1} f_A(x), \quad (45)$$

the CDF of X_{A,N_s} can be expressed as

$$F_{X_{A,N_s}}(x) = 1 - [1 - F_A(x)]^{N_s} \quad (46)$$

where

$$f_A(x) = \frac{1}{\sqrt{2\pi}\sigma_n} e^{-\frac{(x-A)^2}{2\sigma_n^2}}, \quad (47)$$

and

$$F_A(x) = \frac{1}{2} \left[1 + \operatorname{erf} \left(\frac{x-A}{\sqrt{2}\sigma_n} \right) \right]. \quad (48)$$

We define $X = X_{0,1}$, $Y = X_{A,N_s}$. Then we have

$$\begin{aligned} P_{0A} &= \operatorname{Prop}\{X > Y\} \\ &= \int_{-\infty}^{+\infty} dy \int_y^{+\infty} dx f_X(x) f_Y(y) \\ &= \int_{-\infty}^{+\infty} [1 - F_X(y)] f_Y(y) dy \\ &= \mathcal{OR}(0, A, N - N_s, N_s, \sigma_n). \end{aligned} \quad (49)$$

APPENDIX B PROOF OF THEOREM 2

To calculate the BER of RPIM with OSD, we also only consider the case that a pair of error happens. If it happens in the first phase for detecting A_H , the error detection probability is P_{LH} . In this event, the error propagation will happens from the first error to the second error, resulting in that the number of error bits equals $(t_2 - t_1) \log_2 M/2$. The error probability of any pair (t_1, t_2) , $t_2 > t_1$ is $2/[N_s(N_s - 1)]$. Considering the total number of bits is $N_s \log_2 M$, the BER of the first phase can be calculated as the first term of equation (29). Otherwise, it happens in the second phase for detecting A_L . As the detection in the second phase for Q times, and the average BER can be approximated by the error probability of one time detection. For one detection, error propagation exists between the first and the second error and the number of error bits equals $[\mathcal{N}(t_2) - \mathcal{N}(t_1)] \log_2 M/2$. The error detection probability of the second phase for any (t_1, t_2) , $t_2 > t_1$ is $2(1 - P_{LH})/[W(W - 1)]$. The total number of bits in one detection is $(K - 1) \log_2 M$. Thus the mean BER in the second phase can be calculated as the second term in (29). Summarizing all above, Theorem 2 is proved.

REFERENCES

- [1] Z. Ghassemlooy, W. Popoola, and S. Rajbhandari, *Optical wireless communications: system and channel modelling with Matlab*. CRC press, 2012.
- [2] S. Guo, K.-H. Park, and M.-S. Alouini, "Polar coordinate based modulation: Concept, performance analysis and system design," *Proc. of IEEE ICC Wkshps, 2018*, pp. 1–6, Kansas City, MO, USA 2018.
- [3] S. Guo, K.-H. Park, H. Zhang, and M.-S. Alouini, "Polar coordinate based optical (PCO-) OFDM," *submitted to IEEE Trans. Comm.*, 2018.
- [4] M. A. Khalighi and M. Uysal, "Survey on free space optical communication: A communication theory perspective," *IEEE Commun. Surveys Tuts.*, vol. 16, no. 4, pp. 2231–2258, Apr. 2014.
- [5] F. Xu, A. Khalighi, P. Caussé, and S. Bourennane, "Channel coding and time-diversity for optical wireless links," *Opt. Express*, vol. 17, no. 2, pp. 872–887, Jan. 2009.
- [6] S. G. Wilson, M. Brandt-Pearce, Q. Cao, and M. Baedke, "Optical repetition MIMO transmission with multipulse PPM," *IEEE J. Sel. Areas Commun.*, vol. 23, no. 9, pp. 1901–1910, Sep. 2005.
- [7] Z. Ghassemlooy, A. R. Hayes, N. L. Seed, and E. D. Kaluarachchi, "Digital pulse interval modulation for optical communications," *IEEE Commun. Mag.*, vol. 36, no. 12, pp. 95–99, Dec. 1998.
- [8] G. A. Mahdiraji and E. Zahedi, "Comparison of selected digital modulation schemes (OOK, PPM and DPIM) for wireless optical communications," in *2006 4th Student Conference on Research and Development*, Selangor, Malaysia, Jun. 2006, pp. 5–10.
- [9] Z. Ghassemlooy, S. Armon, M. Uysal, Z. Xu, and J. Cheng, "Emerging optical wireless communications—advances and challenges," *IEEE J. Sel. Areas Commun.*, vol. 33, no. 9, pp. 1738–1749, Sep. 2015.
- [10] S. Al-Dharrab, M. Uysal, and T. M. Duman, "Cooperative underwater acoustic communications [accepted from open call]," *IEEE Commun. Mag.*, vol. 51, no. 7, pp. 146–153, Jul. 2013.
- [11] C. Gabriel, M.-A. Khalighi, S. Bourennane, P. Léon, and V. Rigaud, "Investigation of suitable modulation techniques for underwater wireless optical communication," in *Proc. IEEE IWOW*. IEEE, 2012, pp. 1–3.
- [12] V. Chan, "Coding for the turbulent atmospheric optical channel," *IEEE Trans. Commun.*, vol. 30, no. 1, pp. 269–275, Jan. 1982.
- [13] F. M. Davidson and Y. T. Koh, "Interleaved convolutional coding for the turbulent atmospheric optical communication channel," *IEEE Trans. Commun.*, vol. 36, no. 9, pp. 993–1003, Sep. 1988.
- [14] N. Cvijetic, S. G. Wilson, and R. Zarubica, "Performance evaluation of a novel converged architecture for digital-video transmission over optical wireless channels," *J. Lightw. Technol.*, vol. 25, no. 11, pp. 3366–3373, Nov. 2007.
- [15] I. B. Djordjevic, S. Denic, J. Anguita, B. Vasic, and M. A. Neifeld, "LDPC-coded MIMO optical communication over the atmospheric turbulence channel," *J. Lightw. Technol.*, vol. 26, no. 5, pp. 478–487, May 2008.
- [16] H. G. Sandalidis, T. A. Tsiftsis, G. K. Karagiannidis, and M. Uysal, "BER performance of FSO links over strong atmospheric turbulence channels with pointing errors," *IEEE Commun. Lett.*, vol. 12, no. 1, pp. 44–46, Jan. 2008.
- [17] H. G. Sandalidis, T. A. Tsiftsis, and G. K. Karagiannidis, "Optical wireless communications with heterodyne detection over turbulence channels with pointing errors," *J. Lightw. Technol.*, vol. 27, no. 20, pp. 4440–4445, Oct. 2009.
- [18] E. Bayaki, R. Schober, and R. K. Mallik, "Performance analysis of MIMO free-space optical systems in gamma-gamma fading," *IEEE Trans. Commun.*, vol. 57, no. 11, pp. 3415–3424, Nov. 2009.
- [19] E. Zedini, A. Chelli, and M. S. Alouini, "On the performance analysis of hybrid ARQ with incremental redundancy and with code combining over free-space optical channels with pointing errors," *IEEE Photonics Journal*, vol. 6, no. 4, pp. 1–18, Aug. 2014.
- [20] B. Makki, T. Svensson, T. Eriksson, and M. S. Alouini, "On the performance of RF-FSO links with and without hybrid ARQ," *IEEE Trans. Wireless Commun.*, vol. 15, no. 7, pp. 4928–4943, Jul. 2016.
- [21] H.-C. Yang and M.-S. Alouini, *Order statistics in wireless communications: diversity, adaptation, and scheduling in MIMO and OFDM systems*. Cambridge University Press, 2011.